THEORETICAL AND EXPERIMENTAL STUDY OF CdS

K. Ouari, N. Benramdane*, Z. Kebbab*, A. Bouzidi*
H. Tabet-Drraz, R. Desfeux***

[*]Laboratoire d'Elaboration et de caractérisation des matériaux, département d'électronique,
Université Djillali Liabes, BP89, Sidi Bel Abbès, Algérie, E-mail: ouari_k@yahoo.fr

[**]Laboratoire de Physico-Chimie des Interfaces et Applications, Université d'Artois,
Faculté Jean Perrin, Rue Jean Souvraz, SP18, 62307 Lens, France

Received: 1 Oct, accepted: 6 Nov 2007

In the present paper, we investigate theoretically and experimentally the structural and optical properties of wurtzite (WZ) CdS semiconductor. The reflectance and transmittance spectra in the [1.5-3.5] eV range of a thin CdS film prepared by spray pyrolysis has been carried out. The first principles full potential linearized augmented plane wave (FPLAPW) method has been utilized to complete the study.

Keywords: structural materials, photovoltaic effect in semiconductor structures, FPLAPW method, spray pyrolysis technique, wurtzite CdS.

Kheira Ouari

Organization(s): Université de Sidi Bel Abbès.
Education: Université de Sidi Bel Abbès, Faculté des sciences et sciences de l'ingénieur, Engineer (1992-1996), Magister (2001-2004).
Experience: Teaching in university, member in research laboratory.
Main range of scientific interests: microelectronic**,** semiconductor, photo voltaic.
Publications: Theoretical and experimental study of wurtzite CdO (Communication). N. Benramdhane, K. Ouari, Z. Kebbab, A. Bouzidi, H. Boudaoud, R. Desfeux. Drip XI (Beeging chine).

Introduction

Cd-based II-IV semiconductor compounds are of considerable interest due to their applications in solar cells, optical detectors, field effect transistors and optoelectronic devices [1, 2]. Among these materials, CdS thin films are regarded as one of the most promising materials for heterojunction thin film solar cells. Wide bandgap CdS (E_g = 2.4 eV) has been used as a window material together with several semiconductors such as CdTe, Cu_2S, InP and $CuInSe_2$ with 14-16 efficiency [3, 4]. Depending on the growth temperature, it can stabilise in both zinc-blende (below 150 °C) or WZ phases (above 170 °C) [5, 6].
In this work, structural and optical properties of WZ CdS films grown using spray pyrolysis technique have been studied both experimentally and theoretically. This paper describes a combinatoric exploratory approach to bulk and thin film of CdS, combining theory and experimentation.

Experimental details

CdS thin films were prepared on glass substrates by spray pyrolysis technique. The experimental set-up is similar to that described in Ref. [7]. The glass substrates were cleaned with freshly prepared chromic acid, detergent solution and distilled water. The spray solution consisting of 0.05 M $CdCl_2$ and 0.05 M CH_4N_2S were dissolved in bi-distilled water. Compressed air of pressure 6 N/cm^2 was used as a carrier gas with a solution flow of 5 cm^3/min. The substrate temperature was fixed at 350 °C and controlled through a thermocouple (Chrome-Nickel). Structural characterisation was carried out at room temperature in the θ-2θ scan mode using a Rigaku Miniflex diffractometer (Cukα, radiation, λ = 1.5406 Å). Transmittance and reflectance were measured in the wavelength range of [1.5-3.5] eV using a UV-Visible – NIR JASCO type-570 double beam spectrophotometer.

Computational details

Theoretical calculations were performed using the FPLAPW method [8] based on the density-functional theory (DFT) [9, 10]. The exchange-correlation energy of the electrons is described in the local-density approximation (LDA) using the Perdew-Zunger scheme [11] as implemented in the WIEN 97 code [12]. Basis functions were expanded in combinations of spherical harmonic functions inside non-overlapping spheres surrounding the atomic sites (muffin-tin spheres) and in Fourier series in the interstitial region. In the muffin-tin spheres (MTS), the *L*-expansion of the non-spherical

potential and charge density was carried out up to $L_{MAX} = 12$. Consequently, 2554 plane waves have been utilized, and the energy cut off was set such as $R_{MT} \cdot K_{MAX} = 8$ (K_{MAX} being the maximum modulus for the reciprocal lattice vector and R_{MT} is the radius of the MTS). Furthermore, we adopted the value of 1.8 a.u for S and 2 a.u for Cd.

The electronic configuration of CdS is: Cd: [Kr] $4d^{10}5s^2$ and S: [Ne] $3s^23p^4$. In WZ, the Cd atoms are located at (0,0,0), (1/3,2/3,1/2) and the S atoms are located at (0,0,*u*), (1/3,2/3,1/2+*u*). The internal parameter *u* was fixed to the ideal value of a WZ crystal.

Results

Fig. 1 shows the X-ray diffraction pattern of our CdS film which indicates that the deposited film is polycrystalline with a hexagonal WZ structure of spatial group 186 ($P6_3/mc$). The peaks were indexed by comparing our measured inter-reticular distances $d_{(hkl)}$ and their intensities *I* to the 41-104 JCPDS X-ray powder data file. The lattice constants *a* and *c* were determined by using the following quadratic relation:

$$d_{hkl} = \frac{a}{\sqrt{\frac{4}{3}(h^2 + k^2 + hk) + \frac{l^2 a^2}{c^2}}}, \quad (1)$$

and were found to be 4.117 Å and 6.696 Å respectively. These values are in good agreement with previous results [13].

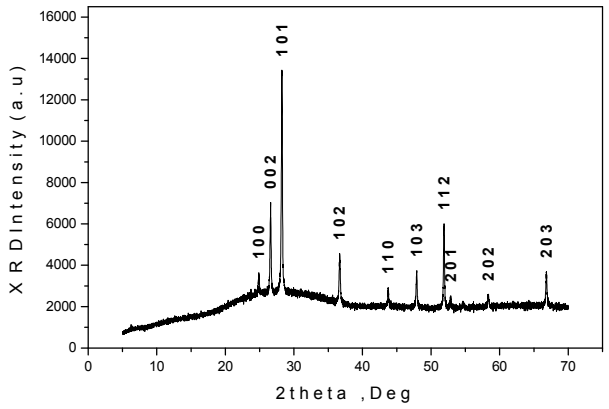

***Fig. 1**. XRD spectra of wurtzite CdS*

For reasons of comparison, we have also calculated theoretically the structural properties of our compound. The total energies were calculated in two steps. First, we varied the *c*/*a* ratio at a fixed volume and a stable *c*/*a* ratio was obtained by a parabolic fit. The equilibrium *c*/*a* value was found to be 1.626. In the second step, we fixed the equilibrium *c*/*a* and we varied the volume which was then fitted to Murnaghan's equation of state [14] as given by:

$$E(v) = \frac{B_0 v}{B_0'}\left[\frac{(v_0/v)^{B_0'}}{B_0' - 1} + 1\right] + cst \quad (2)$$

B and *B*′ being the bulk modulus and its pressure derivative at the equilibrium volume V_0.

Fig. 2 shows the total energy as a function of the volume for wurtzite CdS. The calculated lattice parameters are *a* = 4.108 Å and *c* = 6.679 Å which are found to be less than the experimental values because of LDA. The LDA calculations show a number of systematic shortcomings.

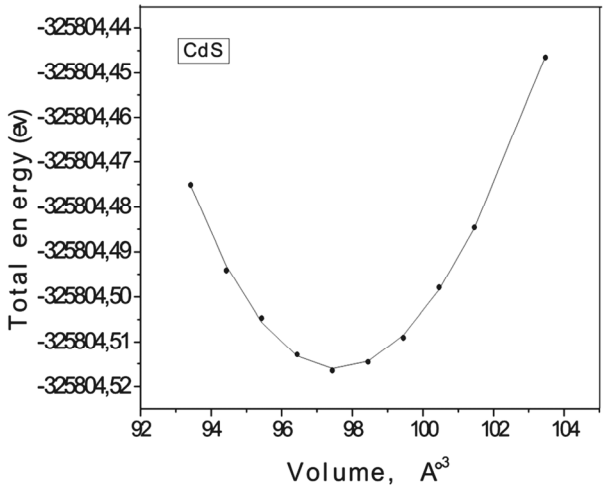

***Fig. 2.** Calculated total energy as a function of volume of CdS*

In the Fig. 3, we show the band structure of CdS obtained by the FPLAPW method. The calculated band gap is found to be only 1 eV. However, the experimental gap of CdS is 2.5 eV [15]. It is well known that the LDA based FLAPW underestimates gaps by 50 % or more, especially for II–VI compound semiconductors [16].

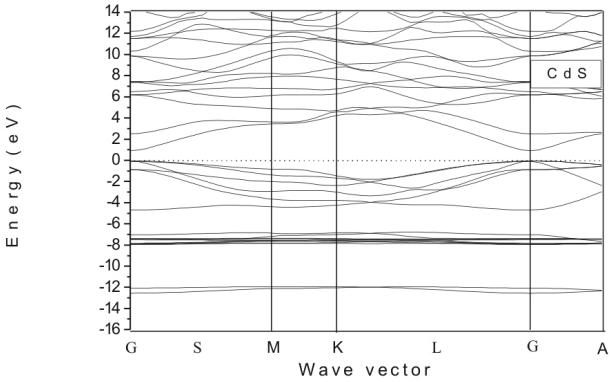

***Fig. 3.** Band structure for CdS in wurtzite structure*

In order to understand the general feature of the bonding in this compound, the total and partial densities of states (DOS and PDOS) integrated over the atoms and the interstitial region outside the MTS are shown in Fig .4.

The total DOS presents three regions: the lower band at around -8 to -7 eV is derived from the cadmium 4*d* states. The bands between -5 eV and the valence band maximum are mostly derived from the S *p*-states hybridised with Cd *s*-states. The states of the conduction band are mainly S *p*-states hybridised with Cd *s*-states with only small admixture of Cd 4*d*-states.

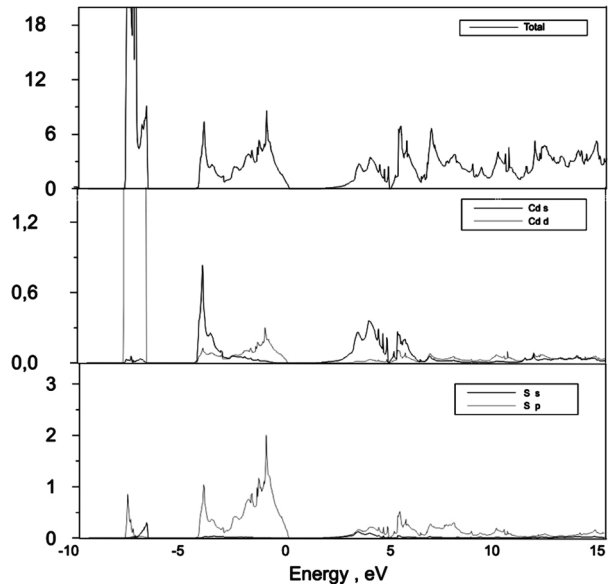

Fig. 4. *Total and partial density of states (DOS and PDOS) for CdS*

The total valence charge density is displayed along the Cd-S bonds and in the (110) plane containing Cd and S atoms (Fig. 5). The charge transfer gives rise to the ionic character of CdS similar to that found in other II-VI compound semiconductors. The driving force behind the displacement of the bonding charge is the greater ability of S to attract electrons towards it due to the difference in the electronegativity between Cd and S.

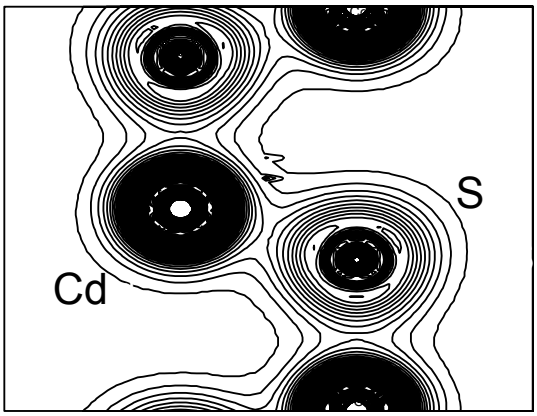

Fig. 5. *Contour plot of the total valence charge density in the (110) plane of CdS*

In order to investigate the optical properties of CdS, we used a mesh of 200 irreducible K points in the Brillouin zone and we shifted the conduction bands. The imaginary part of the dielectric constant $\varepsilon_2(E)$ was calculated by considering summation over all conduction and valence bands and over the first Brillouin zone. The real part $\varepsilon_1(E)$ was then obtained from $\varepsilon_2(E)$ by the use of the Kramers-Kronig relations. The other parameters follow straightforwardly.

Experimentally, optical transmittance and reflectance for CdS film were measured in the range [1.5-3.5] eV using a JASCO V-570 spectrophotometer. Fig. 6 shows the transmittance and reflectance spectra.

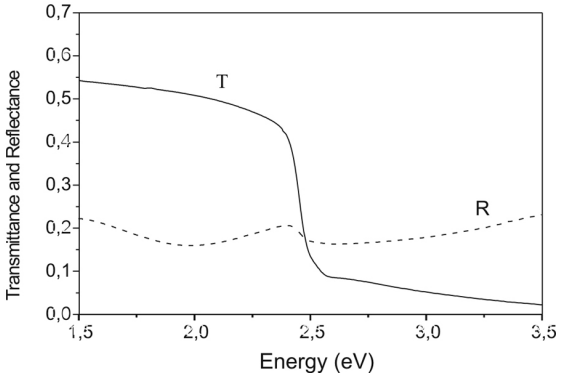

Fig. 6. *Transmittance and reflectance of CdS film*

T is in order of 5 % for higher energies values, and it increases to 50 % for low energy. *R* roughly levels off in the range [1.5, 2.5] eV energy and it increases from 2.5 to 3.5 eV. Similar behaviour in the transmission and reflectance spectra of CdS films prepared by other techniques have been reported in the literature [17-19]. The absorption coefficient α was calculated from the relation [20]:

$$T = \frac{(1-R)^2 e^{-\alpha d}}{R^2 e^{-2\alpha d}}, \qquad (3)$$

R and *T* being the spectral reflectance and transmittance and *d* the film thickness. The value of the energy band gap was calculated using the formula:

$$(\alpha h\nu)^2 = A(h\nu - E_g), \qquad (4)$$

where *A* is a constant which is related to the effective masses associated with the bands and E_g is the bandgap energy. Plot of $(\alpha h\upsilon)^2$ versus the photon energy $h\upsilon$ for film is shown in Fig. 7.

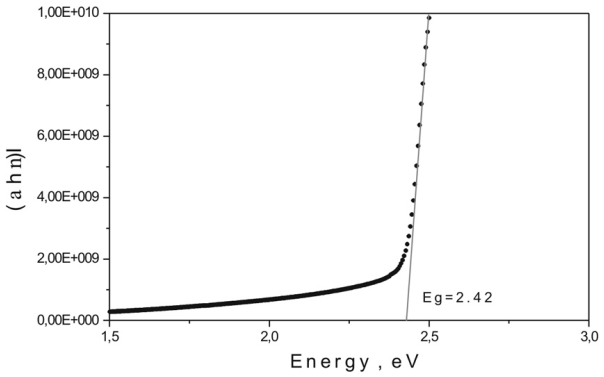

Fig. 7. *$(\alpha h\nu)^2$ vs. $(h\nu)$ plot for CdS film*

The linearity of the plot indicates that the material is of direct band gap nature. Extrapolation of linear portion of the graph to the energy axis at $\alpha = 0$ gives the value of the band gap energy, which is found to be 2.42 eV, in good agreement with Pal et al [21].

Fig. 8, 9 and 10 show the theoretical and experimental curves respectively in [1.5-3.5] eV range.

Fig. 8 shows the theoretical and experimental absorption coefficient. Good agreement is found between theory and measurement. However, due to the polycrystalline structure of the thin film, extra absorption of light occurs at the grain boundaries. This leads to non-zero value of α for photon energies smaller than the fundamental absorption edge.

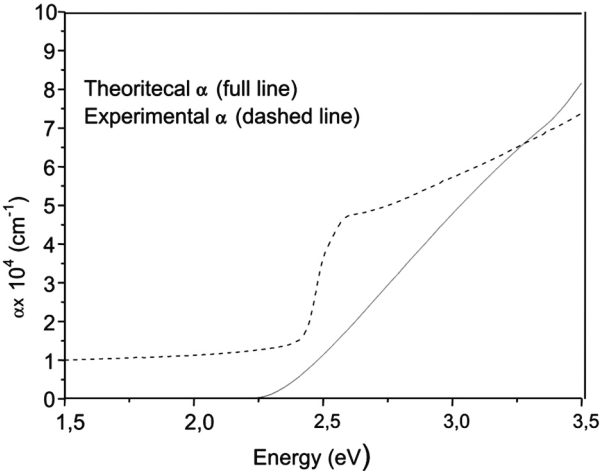

Fig. 8. *Theoretical and experimental α(E)*

In Fig. 9 the theoretical and experimental refractive index are presented. It is observed that for the experimental index there is one well-defined maximum. This observation is accounted to the particular structure of the film and it thickness [22, 23]. The peak value of the experimental of the refractive index is 2.45. The values of theoretical *n* increase with increasing photon energy. The smaller *n* experimental values in the range [2, 3.5] eV may be due to the polycrystalline structure of the film investigated.

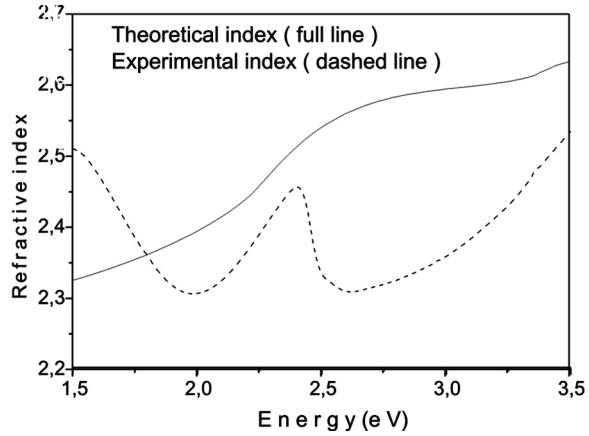

Fig. 9. *Theoretical and experimental n(E)*

Finally, Fig. 10 shows the theoretical and experimental reflectance. A good correspondence of the measured reflectance spectrum and the theoretical model in the range [2.5, 3.5] eV, only minor difference can be observed. Due to the transparency of the film, experimental *R* roughly levels off below 2.5 eV.

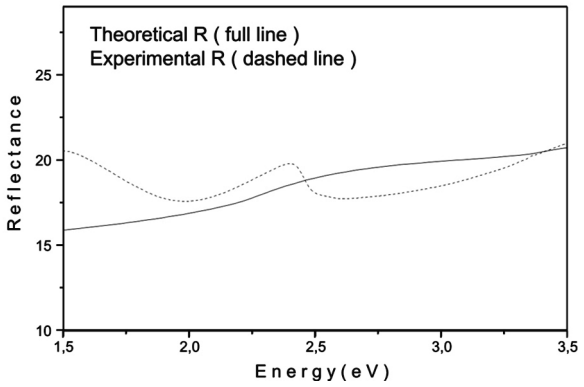

Fig. 10. *Theoretical and experimental R(E)*

Conclusion

In summary, we have presented a study of structural and optical properties of bulk and thin film of WZ CdS. The main conclusion can be summarized as follows:

– WZ CdS is a semiconductor with a direct optical band gap of about 2.42 eV witch is located at the Γ point of the BZ.

– The density of states on both sides of the gap has predominantly *s-p* character with only small admixture of *s*-states.

– The calculated electron charge distribution indicates an ionic character.

– The film exhibit high transmittance (more than 50 %) and low reflectance in the visible-near infrared region (2.48, 1.127) eV region, making the film suitable for optoelectronic devices, for instance as window layers in solar cells.

– The absorption coefficient α and refractive index *n* values ad reflectance *R* using the optical measurement are found to agree well with the results obtained using theoretical calculations.

References

1. Das S., Datta S.K., Saka H. Structure of vacuum, evaporated $Cd_xZn_{1-x}S$ thin films // Phys. Stat. Sol. 1993. Vol. a, No. 136. P. 251.

2. Touskova J., Kindl D., Tousek J. Preparation and characterization of CdS/CdTe thin film solar cells // Thin Solid Films // Phys. Stat. Sol. 1997.Vol. 293, No.142. P. 272-276.

3. Su B., Choy K.L. Growth behavior and microstructure of CdS thin films deposited by an electrostatic spray assisted vapor deposition (ESAVD) process // Thin Solid Films. 2001. Vol. 338. P. 9-14.

4. Wu X., Keane J.C., DeHart R.G., Albin D.S., Duda A., Gessert T.A., Asher S., Levi D.H., Sheldon P. Proceeding of the 17th European Photovoltaic Solar Energy Conference, Munich, Germany, 2001. P. 995.
5. Landolt-Bornstein: Numerical Data and Functional Relationships in science and technology, edited by O. Madelung, M. Schultz, and H. Weiss (Springer–Verlag, Berlin, 1982). Vol. 17b.
6. Vankar V.D., Das S.R., Prem Nath, Chopra K.L. Structure of vacuum, evaporated $Cd_xZn_{1-x}S$ thin films // Phys. Stat. Sol. 1978. Vol. 45. P. 665-669.
7. Chalapathy R.B.V. PhD Thesis, Sri Venkateswara University, Tirupati, India, 2001.
8. Jansen H.J.F., Freeman A.J. Total-energy full-potential linearized augmented-plane-wave method for bulk solids: Electronic and structural properties of tungsten // Phys. Rev. 1984. Vol. B, No. 30. P. 561.
9. Hohenberg P., Kohn W. One-particle properties of an inhomogeneous interacting electron gas // Phys. Rev. 1964. Vol. B, No. 136. P. 864.
10. Sham L.J., Kohn W. One-particle properties of an inhomogeneous interacting electron gas // 1965. Vol. B, No. 145. P. 561.
11. Perdew J.P., Wang Y. Accurate and simple analytic representation of the electron-gas correlation energy // Phys. Rev. 1992. Vol. B, No. 45. P. 13244.
12. Blaha P., Schwarz K., Luitz J. WIEN97, Vienna University of Technology, Vienna, 1997.
13. Razik N., Mater J. Use of a standard reference material for precise lattice parameter determination of materials of hexagonal crystal structure // Sci. Lett. 1987. Vol. 6, No. 12. P. 1443.
14. Murnaghan F.D. The compressibility of media under extreme pressures // 1944. Vol. 30. P. 244-247.
15. Polmann Johannes, Vogel Dirk., Krüger Peter. Self-interaction and relaxation-corrected pseudopotentials for II-VI semiconductors // Phys. Rev. 1996. Vol. B, No. 54. P. 5495.
16. Cardona M., Christensen N.E., Lew Yan Voon L.C., Willatzen M. Terms linear in k in the band structure of wurtzite-type semiconductors // Phys. Rev. 1996. Vol. B, No. 53. P. 10703.
17. Moon Byung-Sik, Lee Jae-Hyeong, Jung Hakkee. Comparative studies of the properties of CdS films deposited on different substrates by R.F. sputtering // Thin Solid Films. 2006. Vol. 511-512. P. 299-303.
18. Senthil K., Mangalaraj D., Narayandass Sa., Adachi Sadao. Mat. Sci. Eng. B 78, 53 (2000).
19. Achour A., Al-kadry N., Mahmoud S.A. Defect distribution in electron-irradiated CdS materials // Thin Solid Films. 1995. Vol. 238. P. 110-114.
20. El Manduh Z.S., Selim M.S. Physical properties of vanadium pentoxide sol gel films // Thin Solid Films. 2000. Vol. 371. P. 259-263.
21. Pal U., Silva-Gonzalez R., Martinez-Montes G., Gracia-Jemenez M., Vidal M., Torres S. Optical characterization of vacuum evaporated cadmium sulfide films // Thin Solid Films. 1997. Vol. 345. P. 345-350.
22. Yamaguchi K., Nakayama N., Matsumoto H., Iegami S. 8.5 % efficient screen-printed CdS/CdTe solar cell produced on a 5×10 cm^2 glass substrate // Appl. Phys. 1977. Vol. 16. P. 1203.
23. Tepehan F., Ozer N. Sol. En. Mater. // Sol Cells 30, 353 (1993).